REPORT DOCUMENTATION PAGE

Form Approved OMB NO. 0704-0188

1. REPORT DATE (DD-MM-YYYY)	2. REPORT TYPE	3. DATES COVERED (From - To)
17-06-2008	Final Report	15-May-2004 - 14-May-2007

4. TITLE AND SUBTITLE
Damping MEMS Devices in Harsh Environments Using Active Thin Films

5a. CONTRACT NUMBER
W911NF-04-1-0193

5b. GRANT NUMBER

5c. PROGRAM ELEMENT NUMBER
611102

6. AUTHORS
Greg P. Carman, Catherine A. Kerrigan

5d. PROJECT NUMBER

5e. TASK NUMBER

5f. WORK UNIT NUMBER

7. PERFORMING ORGANIZATION NAMES AND ADDRESSES
University of California - Los Angeles
The Regents of The University of California, Los Angeles
11000 Kinross Avenue, Suite 102
Los Angeles, CA 90095 -1406

8. PERFORMING ORGANIZATION REPORT NUMBER

9. SPONSORING/MONITORING AGENCY NAME(S) AND ADDRESS(ES)
U.S. Army Research Office
P.O. Box 12211
Research Triangle Park, NC 27709-2211

10. SPONSOR/MONITOR'S ACRONYM(S)
ARO

11. SPONSOR/MONITOR'S REPORT NUMBER(S)
45555-EG.4

12. DISTRIBUTION AVAILIBILITY STATEMENT
Approved for Public Release; Distribution Unlimited

13. SUPPLEMENTARY NOTES
The views, opinions and/or findings contained in this report are those of the author(s) and should not contrued as an official Department of the Army position, policy or decision, unless so designated by other documentation.

14. ABSTRACT
We report on fabrication and damping measurment of NiTi and Terfenol-D thin films. A model for prediction of the damping properties (tan delta) of a laminate using the material properties of the layers was developed. Damping properties in Nitinol thin film due only to residual stresses was measured to be as high as tan delta = 0.17 for large strain (0.9%). At lower strain levels a Nitinol/Silicon laminate was tested in a cantilever load frame. The damping value of the film was measured to be 0.28 (at 0.27% strain). A Nitinol/Terfenol-D/Nickel laminate was fabricated and tested in a cantilever loading. The damping value of the film was measured to be 0.2 (at 0.27% strain).

15. SUBJECT TERMS
thin film damping terfenol-d nitinol

16. SECURITY CLASSIFICATION OF:			17. LIMITATION OF ABSTRACT	15. NUMBER OF PAGES	19a. NAME OF RESPONSIBLE PERSON
a. REPORT	b. ABSTRACT	c. THIS PAGE			Gregory Carman
U	U	U	SAR		19b. TELEPHONE NUMBER 310-825-6030

Report Title

Damping MEMS Devices in Harsh Environments Using Active Thin Films

ABSTRACT

We report on fabrication and damping measurment of NiTi and Terfenol-D thin films. A model for prediction of the damping properties (tan delta) of a laminate using the material properties of the layers was developed. Damping properties in Nitinol thin film due only to residual stresses was measured to be as high as tan delta = 0.17 for large strain (0.9%). At lower strain levels a Nitinol/Silicon laminate was tested in a cantilever load frame. The damping value of the film was measured to be 0.28 (at 0.27% strain). A Nitinol/Terfenol-D/Nickel laminate was fabricated and tested in a cantilever loading. The damping value of the film was measured to be 0.2 (at 0.27% strain).

List of papers submitted or published that acknowledge ARO support during this reporting period. List the papers, including journal references, in the following categories:

(a) Papers published in peer-reviewed journals (N/A for none)

Cole, M., Nothwang, W., Hirsch, S., Mohanchandra, K.P., Demaree, J., and Carman G.P., "Integration of Active Thin Films with Silicon Compatible Materials and Process Science Protocols for MEMS Scale Vibration Damping Applications," Integrated Ferroelectrics, V71, 2005, pp. 81-98.

Mohanchandra, K.P., Ho, K.K., Carman, G.P., "Compositional uniformity in sputter-deposited NiTi shape memory alloy thin films," Materials Letters, V62, 20, pp. 3481-3483.

Number of Papers published in peer-reviewed journals: 2.00

(b) Papers published in non-peer-reviewed journals or in conference proceedings (N/A for none)

Number of Papers published in non peer-reviewed journals: 0.00

(c) Presentations

Number of Presentations: 0.00

Non Peer-Reviewed Conference Proceeding publications (other than abstracts):

Catherine Kerrigan, Ken K. Ho, K.P. Mohachandra, Gregory P. Carman, “Microscale Damping Using Thin Film Active Materials,” Proceedings of SPIE – the International Society of Optical Engineering. Vol. 6525, 65250V, 2007.

Catherine Kerrigan, K.P. Mohachandra, Gregory P. Carman, Passive damping of thin film Nitinol,” Proceedings of SPIE – the International Society of Optical Engineering. Vol. 6169, 2006, pp. 138-147.

D. A. Ruggles, G. P. Carman, “Damping of polycrystalline ferromagnetic shape alloy bulk and sputtered thin film,” Presented at SPIE International Symposia Smart Structures & Materials/NDE, San Diego, California USA, March 2005

Ruggles, D.A., Gans, E., Mohanchandra K.P., Carman, G.P., Ngo, E., Nothwang, W., Cole, M.W., “Damping of polycrystalline Ni-Mn-Ga, bulk, PLD, and sputtered thin film,” Proceedings of SPIE – the International Society of Optical Engineering. Vol. 5387, 2004, pp. 156-163.

Number of Non Peer-Reviewed Conference Proceeding publications (other than abstracts): 4

Peer-Reviewed Conference Proceeding publications (other than abstracts):

Number of Peer-Reviewed Conference Proceeding publications (other than abstracts): 0

(d) Manuscripts

CA Kerrigan, KK Ho, KP Mohachandra, GP Carman, “Sputter deposition and analysis of thin film NiTi/Terfenol-D multilaminate for vibration damping.” Smart Materials and Structures, 2008, Submitted.

Number of Manuscripts: 1.00

Number of Inventions:

Graduate Students

NAME	PERCENT_SUPPORTED
David Ruggles	0.50
Catherine Kerrigan	0.50
FTE Equivalent:	**1.00**
Total Number:	**2**

Names of Post Doctorates

NAME	PERCENT_SUPPORTED
Mohanchandra Kotekar Panduranga	0.10
FTE Equivalent:	**0.10**
Total Number:	**1**

Names of Faculty Supported

NAME	PERCENT_SUPPORTED	National Academy Member
Greg Carman	0.05	No
FTE Equivalent:	**0.05**	
Total Number:	**1**	

Names of Under Graduate students supported

NAME	PERCENT_SUPPORTED
Sam Sandoval	0.00
FTE Equivalent:	**0.00**
Total Number:	**1**

Student Metrics

This section only applies to graduating undergraduates supported by this agreement in this reporting period

The number of undergraduates funded by this agreement who graduated during this period:	1.00
The number of undergraduates funded by this agreement who graduated during this period with a degree in science, mathematics, engineering, or technology fields:.....	1.00
The number of undergraduates funded by your agreement who graduated during this period and will continue to pursue a graduate or Ph.D. degree in science, mathematics, engineering, or technology fields:.....	1.00
Number of graduating undergraduates who achieved a 3.5 GPA to 4.0 (4.0 max scale):	1.00
Number of graduating undergraduates funded by a DoD funded Center of Excellence grant for Education, Research and Engineering:	0.00
The number of undergraduates funded by your agreement who graduated during this period and intend to work for the Department of Defense	0.00
The number of undergraduates funded by your agreement who graduated during this period and will receive scholarships or fellowships for further studies in science, mathematics, engineering or technology fields:	1.00

Names of Personnel receiving masters degrees

NAME
David Ruggles
Total Number: 1

Names of personnel receiving PHDs

NAME
Catherine Kerriga (expected)
Total Number: 1

Names of other research staff

NAME	PERCENT_SUPPORTED
FTE Equivalent:	
Total Number:	

Sub Contractors (DD882)

Inventions (DD882)

Damping MEMS Devices in Harsh Environments Using Active Thin Films

Greg P. Carman and Catherine A. Kerrigan

Project: W911NF-04-1-0193

University of California at Los Angeles, Mechanical & Aerospace Engineering Department
38-137M Engineering IV, 420 Westwood Plaza, Los Angeles, CA 90024

Table of Contents

List of Figures

Objective

The objective of this program is to understand and develop a new approach to dampen micro-electrical-mechanical-systems (MEMS) structures in harsh environments. The new approach relies on thin film active materials to absorb energy passively through domain wall or twin boundary motion. Damping is required in many military MEMS components used in harsh environments where accuracy and survivability are critical concerns. Typically, MEMS components are used in sensors to provide information on position, velocity, and acceleration, or

are used in communication systems such as phased array antennas. However, when MEMS components are used in military harsh and rugged environments (e.g. munitions or antennas) they are prone to failure, fatigue, and inaccuracies due to extreme mechanical vibrations. While current macroscale damping approaches rely on viscoelastic materials, viscoelastic materials are unsuitable for integration in micro devices. Published microscale damping methods include thermoelastic damping, air damping, squeeze film damping, viscous energy dissipation, and constrained layer damping. However all of these approaches provide marginal damping in the microscale and thus new approaches must be developed. The approach being pioneered under this funding at UCLA is the passive use of active materials for thin film damping using the natural motion of domain walls and twin boundaries to absorb the energy. Therefore, the focus of this research is to develop new microscale damping techniques applicable to MEMS sensors to support future military operations.

Manufacturing

Nitinol and Terfenol-D were sputter deposited using a Denton High Vacuum DC magnetron sputtering system. Details on the sputtering system used in this study can be found in [1]. While a number of different systems were evaluated, we present a description of a subset in this report. The thin film is deposited onto a 100mm diameter silicon (100) wafer with 500 nm of wet thermal oxide layer. The Free Standing Zone Melt Terfenol-D target composition of $Tb_{.33}Dy_{0.67}Fe_{1.92}$ (atomic ratio 0.33Tb:0.67Dy:1.92Fe) was acquired from Etrema while the Nitinol target composition of $Ti_{52}Ni_{48}$ (48% Ni by atomic weight) was acquired from SCI Engineered Materials. The Nitinol film was produced using a Ar pressure of 2x10-8 Torr, substrate-to-target distance of 0.04 cm, and dc power of 300 Watts [1]. Different process

parameters were used to produce thin films of Fe-Tb-Dy. The DC power was varied from 60 to 400 Watts and Ar pressure was varied from $1.5x10^{-3}$ to $1.5x10^{-2}$ Torr. In all these cases the as grown Fe-Tb- Dy films were amorphous. Different annealing temperatures and time were used to crystallize the film. The temperature was measured with a type K thermocouple located at the heating element. The radiatively heated silicon substrate is 0.5cm from the heating element suggesting the actual film temperature is 150°C lower than the thermocouple reading.

Once acceptable fabrication processes were developed for the Terfenol-D thin films, multilayer laminate structures were fabricated. The particular laminates discussed in this report follow. First a Nitinol/Silicon/Nitinol laminate was produced. Ten microns of Nitinol film was sputter deposited on either side of a 100 micron silicon beam (5 mm x 35 mm) and annealed. A second laminate made up of Nitinol, Terfenol-D and Nickel was also produced. The Terfenol-D film was sputter deposited on a nickel beam (5 mm x 35 mm) already coated with crystallized Nitinol film. After crystallizing the Terfenol-D film a second layer of Nitinol was deposited on top of the Terfenol-D layer and subsequently crystallized. This process was repeated on both sides of the Nickel beam. Each Nitinol layer was 3.5μm thick, each Terfenol-D layer was 6.5μm thick and the Nickel layer was 100μm thick.

Annealed films are characterized for their crystallinity by using a PAN Analytical X'pert Pro powder diffractometer. A JEOL electron microprobe with WDS (Wavelength Spectrometry) capability was used to determine Terfenol-D compositions. Magnetic properties were measured using a Quantum Design Model: MPMS XL Superconducting Quantum Interference Device (SQUID). A DSC provides transformation temperatures of the Nitinol film

Nitinol film was tested in a Q800 Dynamic Mechanical Analyzer (DMA) using thin film tension grips. The film is griped on one end while the other end is loaded sinusoidally in tension.

A strain sweep was preformed with strain amplitudes from near zero to 1.0% strain at a frequency of 1Hz at room temperature. Multilayer laminate beam samples were also tested in a Q800 DMA using cantilever beam grips. The sample is clamped at one end while the other end is sinusoidally oscillated. For the purpose of this report, a strain sweep was preformed with strain amplitudes from near zero to ±1.0% strain (a full load reversal) at a frequency of 1Hz at room temperature. Data measured was damping in terms of tan δ, where δ is defined as the lag between stress and strain.

Model of Laminate Damping

An analytical model was developed to predict damping behavior of a multilayered laminate. Each layer has a distinct tan δ and is related to the storage (χ') and loss modulus (χ") as shown in equation 1.

$$\tan\delta = \frac{\chi''}{\chi'} \tag{1}$$

Where χ is defined as a general linear elastic modulus for an orthotropic material (i.e. $\chi = E_1, E_2, E_3, G_{12}, G_{23}, G_{31}$). While the material elastic response can be orthotropic, the following development assumes that damping is isotropic. Storage and loss modulus can also be expressed in terms of tan δ and modulus (equation (2)).

$$\chi' = \frac{\chi}{\sqrt{1+\tan^2\delta}} \qquad \chi'' = \frac{\chi\tan\delta}{\sqrt{1+\tan^2\delta}} \tag{2}$$

Where tan δ is assumed to be small (tan δ < 1) and constant. The modulus (χ) of each layer can be written in terms of its real (storage modulus) and imaginary (loss modulus) components.

$$\chi = \chi' + i\chi'' \tag{3}$$

For plane stress the reduced compliance matrix (S) of an orthotropic material is

$$\left[S_{ij}\right]=\begin{bmatrix} \frac{1}{E_1'+iE_1''} & \frac{-\nu_{21}}{E_2'+iE_2''} & 0 \\ \frac{-\nu_{21}}{E_2'+iE_2''} & \frac{1}{E_2'+iE_2''} & 0 \\ 0 & 0 & \frac{1}{G_{12}'+iG_{12}''} \end{bmatrix}=\left[S'\right]+i\left[S''\right] \tag{4}$$

Where S' and S" are the real and imaginary components of the compliance matrix. Strain (ε) is related to stress (σ) by

$$\left\{\sigma\right\}=\left\{\varepsilon\right\}\left[Q'\right]+i\left\{\varepsilon\right\}\left[Q''\right] \tag{5}$$

Where, [Q'] = $[S']^{-1}$ and [Q"] =$[S"]^{-1}$. Assuming small strains (linear elasticity), perfect bonding between layers and that shearing strains in planes perpendicular to the middle surfaces are negligible ($\gamma_{xz} = \gamma_{yz} = 0$). The strains in the layered system can be expressed as a function of distance (see figure 3-2) from the midplane (z) by

$$\left\{\varepsilon\right\}=\left\{\varepsilon^o\right\}+z\left\{\kappa\right\} \tag{6}$$

Using equation (6) in equation (5), the resultant forces and moments acting on a layered system containing n layers are obtained by integrating the stresses in each layer though the laminate thickness.

$$\left\{N\right\}=\int_{-t/2}^{t/2}\left\{\sigma\right\}dz=\sum_{k=1}^{n}\int_{z_{k-1}}^{z_k}\left\{\sigma\right\}_k\,dz \tag{8}$$

$$\left\{M\right\}=\int_{-t/2}^{t/2}\left\{\sigma\right\}z\,dz=\sum_{k=1}^{n}\int_{z_{k-1}}^{z_k}\left\{\sigma\right\}_k\,z\,dz \tag{9}$$

Where, N is the force per unit width of the cross section of the laminate, M is the moment per unit width. The z_k terms are the distance of each lamina interface from the middle-surface; z_0 defines the top surface and z_n defines the bottom surface (Figure 1).

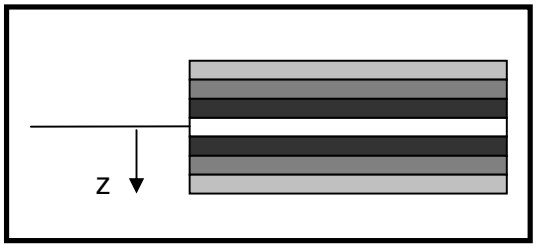

Figure 1: General dimensions for Classic Laminate Theory.

Using the stress-strain relationships (equation (7)) and the applied loads and moments (equation (8) and (9)) relations since midplane strain (ε^o) and midplane curvature (κ) are independent of z the resultant force and moment equations can be rewritten as

$$\begin{Bmatrix} N \\ M \end{Bmatrix} = \begin{bmatrix} A' & B' \\ B' & D' \end{bmatrix} \begin{Bmatrix} \varepsilon^o \\ \kappa \end{Bmatrix} + i \begin{bmatrix} A'' & B'' \\ B'' & D'' \end{bmatrix} \begin{Bmatrix} \varepsilon^o \\ \kappa \end{Bmatrix} \tag{11}$$

$$A'_{ij} = \sum_{k=1}^{N} \left(Q'_{ij}\right)_k \left(z_k - z_{k-1}\right) \qquad A''_{ij} = \sum_{k=1}^{N} \left(Q''_{ij}\right)_k \left(z_k - z_{k-1}\right)$$

$$B'_{ij} = \frac{1}{2} \sum_{k=1}^{N} \left(Q'_{ij}\right)_k \left(z_k^2 - z_{k-1}^2\right) \qquad B''_{ij} = \frac{1}{2} \sum_{k=1}^{N} \left(Q''_{ij}\right)_k \left(z_k^2 - z_{k-1}^2\right)$$

$$D'_{ij} = \frac{1}{3} \sum_{k=1}^{N} \left(Q'_{ij}\right)_k \left(z_k^3 - z_{k-1}^3\right) \qquad D''_{ij} = \frac{1}{3} \sum_{k=1}^{N} \left(Q''_{ij}\right)_k \left(z_k^3 - z_{k-1}^3\right)$$

For isotropic layers where the poisson's ratio of each layer similar (e.g. Terfenol-D and NiTi), the complex Young's modulus for the laminate (E_L) reduces to

$$E_L = \frac{1}{\left(a'_{11} + i a''_{11}\right)\left(z_n - z_0\right)} = \frac{1}{z_n - z_0} \sum_{i=1}^{n} \left(E'_i + i E''_i\right)\left(z_i - z_{i-1}\right) \tag{12}$$

Where, $[a] = [A]^{-1}$. Using equation (1), tan δ of the laminate can also be expressed in terms of Storage and Loss Modulus of each layer (equation (13)).

$$\tan\delta = \frac{E''_L}{E'_L} = \frac{\sum_{i=1}^{n} E''_i \left(z_i - z_{i-1}\right)}{\sum_{i=1}^{n} E'_i \left(z_i - z_{i-1}\right)} \tag{13}$$

Equations (12) and (13) are valid for axial loading only; a different set of equations must be developed for bending. To predict damping properties from bending measurements (i.e. DMA), the D components of the ABD matrix are used. For layups with isotropic layers and similar Poisson's ratio, the complex Young's Modulus in bending reduces to

$$E_L = \frac{12}{\left(d'_{11} + id''_{11}\right)\left(z_n - z_0\right)^3} = \frac{4}{\left(z_n - z_0\right)^3}\left\{\sum_{i=1}^{n}\left(E'_i + iE''_i\right)\left(z_i^3 - z_{i-1}^3\right)\right\} \tag{14}$$

Where, $[d] = [D]^{-1}$. Using equation (1), tan δ of the laminate can also be expressed in terms of Storage and Loss Modulus of each layer (equation (15)).

$$\tan\delta = \frac{E''_L}{E'_L} = \frac{\sum_{i=1}^{n} E''_i\left(z_i^3 - z_{i-1}^3\right)}{\sum_{i=1}^{n} E'_i\left(z_i^3 - z_{i-1}^3\right)} \tag{15}$$

Results and Discussion

Terfenol-D Processing

Before examining damping properties it is necessary to discuss the processing approach for thin film Terfenol-D. A series of thin film characterization techniques are used to evaluate deposited film's composition, crystallography, microstructure, and magnetic properties as a function of deposition parameters. This is important because processing will influence domain wall motion and subsequently damping properties. NiTi deposition and characterization is discussed in detail in reference [1].

WDS measurements were taken for a Terfenol-D film deposited at 100W sputtering power, 10mTorr Ar pressure and a target to substrate distance of 4cm (100W10Ar4cm). Results show the thin film composition is 75at%Fe, 8.3at%Tb and 16.6at% Dy, compared to the measured composition of 66at%Fe, 11at%Tb, 23at%Dy for the target. The deposited film has substantially larger Fe content than Terfenol-D. For material with compositions richer in iron

than $RFe_{1.95}$, RFe_3 precipitates have been shown to form [2-4]. Such precipitates form as narrow plates in the {111} planes of the matrix and potentially impede domain rotation thus decreasing both the magnetostrictive effect and potentially the damping. To reduce the Fe component the sputtering parameters were modified.

Figure 2 shows the results of argon gas pressure on composition. The deposition parameters were 100 W, 4 cm distance, and annealing at 875°C for 15 minutes. The results show that as the sputtering pressure is increased the Fe composition decreases and converges to the target values which are desirable for this study. At argon pressures of 15 mTorr, the Fe composition was 67at%, which is very near the 66.4at% composition of Terfenol-D. In addition to argon pressure, sputtering power was varied from 80 W to 400 W. While the results are not shown here, the Fe content changed by only 3.4at% over this range which was considered inconsequential. Therefore sputtering power did not significantly change film composition and was held fixed at 100W for the damping studies.

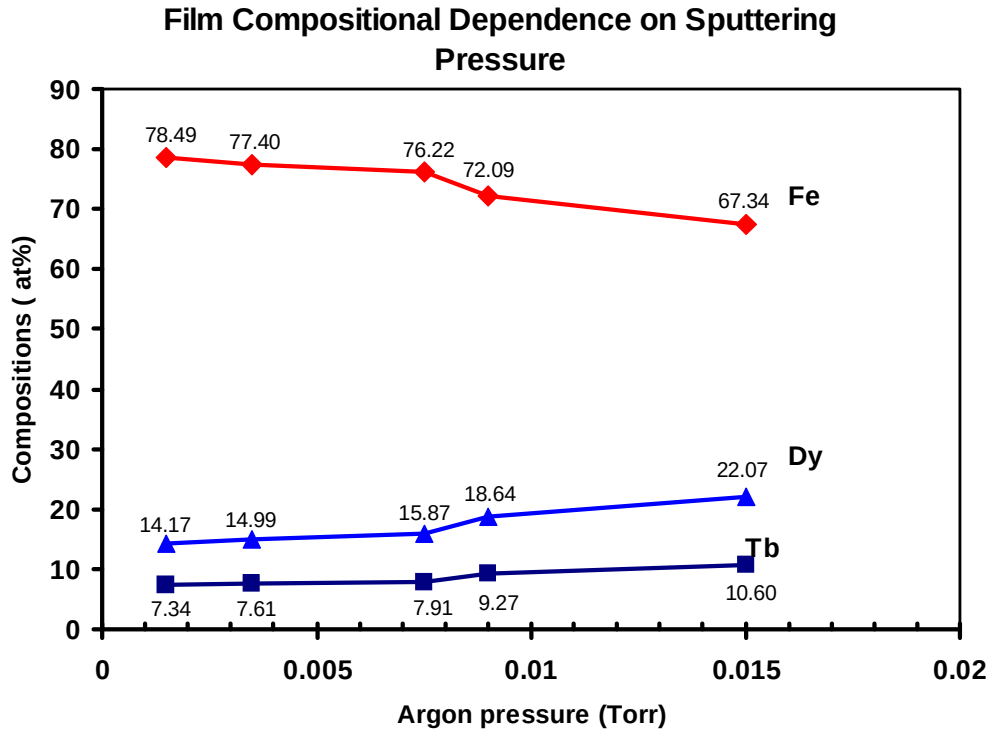

Figure 2: Film composition as a function of sputtering pressure. a) film composition at center of wafer, b) compositional uniformity across diameter of the substrate.

Figure 3 shows XRD plots of the deposited film sputtered at 80W-15mTorr Ar and annealed at 875°C for 5, and 15 minutes. Annealing times of 30 and 120 minutes were also studied but not shown here for brevity.

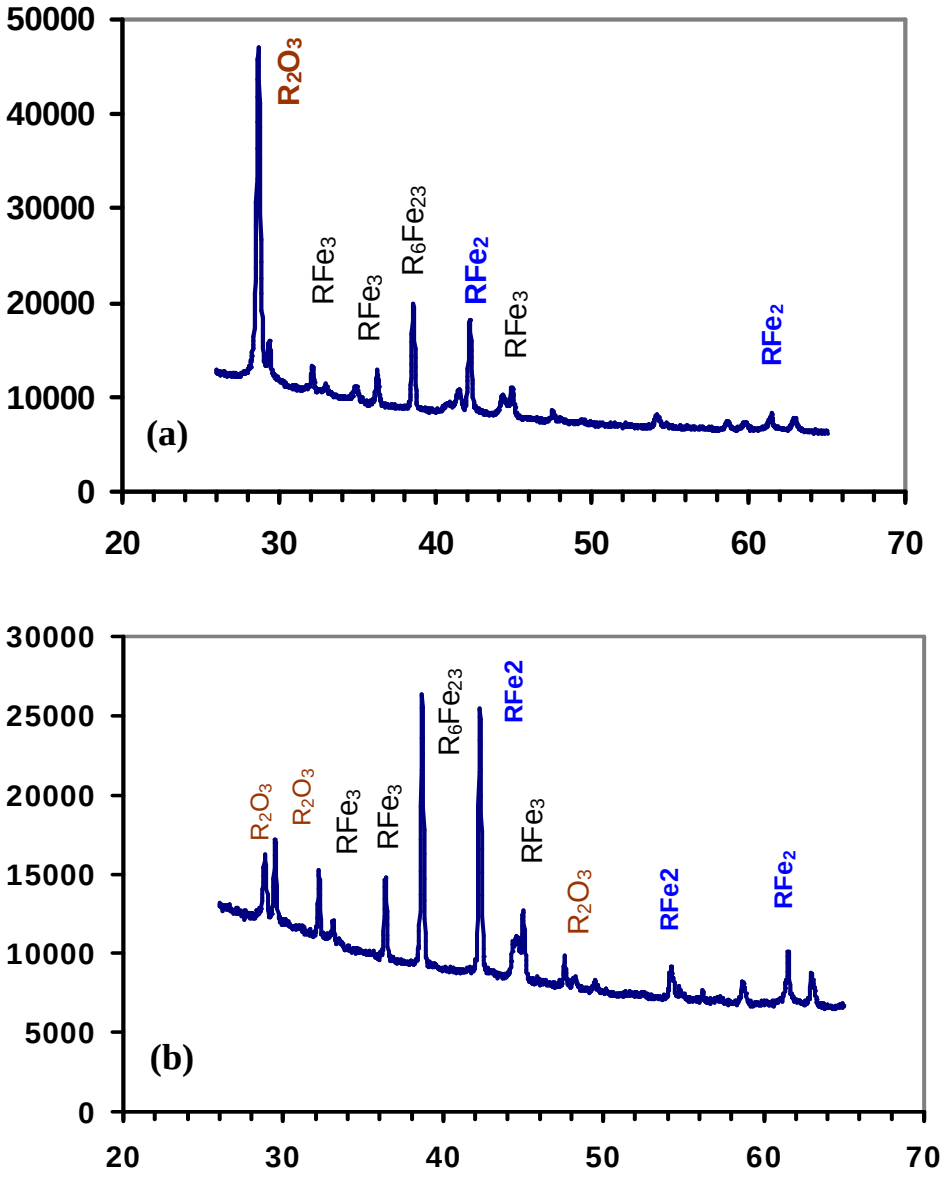

Figure 3: XRD plots of Terfenol-D film under varying annealing times. a) 5 minutes b) 15 minutes at 875°C

Figure 3a shows a 5 minute anneal produces relatively higher oxide peak at $2\theta = 28°$ compared to a 15 minute anneal in Figure 3b. The 28 degree peak in Figure 3a corresponds to unwanted R_2O_3 i.e. a rare earth oxide. When the film is annealed longer than 15 minutes, the oxide peak again predominates, and at 120 minutes of annealing (not shown) this oxide peak far over

shadows other peaks. This indicates that an oxide layer forms fairly quickly (i.e. after 5 minutes). At 15 minutes the desired RFe_2 phase predominates as indicated by the higher intensities at 2θ = 48 and 33° in Figure 3b. However with greater annealing times (i.e. 30 minutes), the oxide peak again predominates. This indicates that 15 minutes annealing is sufficient to crystallize the film with relatively minimal oxides. In addition to studies of annealing time, annealing temperature was also evaluated. Three different annealing temperatures were studied; 750°C, 820°C, and 875°C (i.e. $\approx$ 600°C, 670°C and 725°C at substrate) at a fixed time of 15 minutes. At 750°C the film did not fully crystallize, while at higher temperatures of 820°C and 875°C there were minimal oxide peaks and high RFe_2 peaks. Films used in this damping study were annealed at 875°C (i.e. 725°C at substrate).

Figure 4 plots magnetization versus applied field for the Terfenol-D target and for two thin film Terfenol-D samples. The films were produced with 100W power in either a 1.5mTorr or 15mTorr argon pressure (i.e. indicated on figure 5) and annealed at 875°C from 15 minutes. The saturation magnetization of 0.6 Tesla for the film samples compares favorably with that of the target material of about 0.9 Tesla. However the hysteresis of both thin film samples is substantially larger than the bulk material. This is attributed to oxides pinning the domains. While this increased hysteresis may be an undesirable actuation attribute, it maybe desirable for damping. In particular the 15mTorr sample produced the greatest hysteresis. In addition the remnant magnetization exhibited by the deposited film indicates the possible presence of unreacted and undesirable Fe.

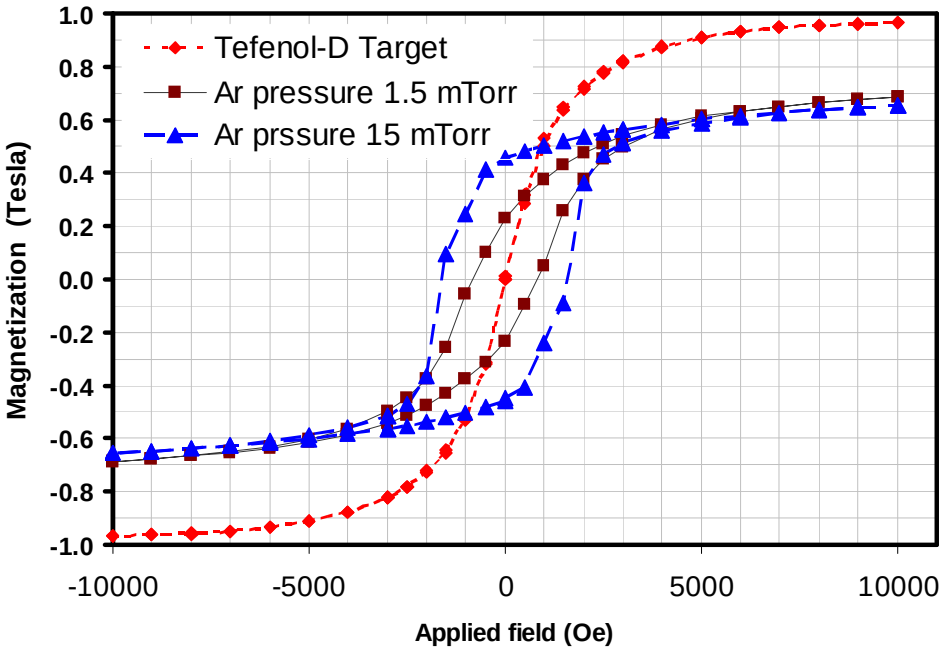

Figure 4: Magnetization versus applied field plots for a) deposited Terfenol-D film b) the Terfenol-D target and c) published values from Wun-Fogle et al.1999 [10].

Damping Results

Figure 5 provides DMA experimental results for dynamic testing of the NiTi film sample in tensile loading. A plot of tan δ versus strain amplitude at room temperature is presented. Tests were preformed at room temperature and a frequency of 1Hz. Figure 5 illustrates the strain dependency of the damping mechanism. At larger strain amplitudes larger tan δ values are measured with values ranging from 0.06 to at 0.25% strain to 0.17 at 0.9% strain.

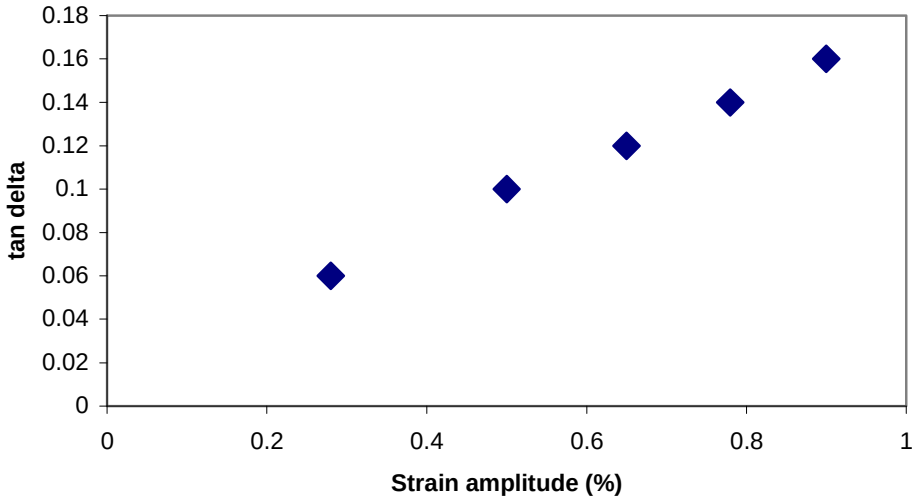

Figure 5: tan δ versus strain amplitude.

Figure 6 and Figure 7 show storage modulus and tan δ respectively versus temperature over a range of 30°C to 100°C for dynamic testing of the thin film NiTi. In this experiment the sample was oscillated at constant strain amplitude of 0.2% while the temperature was stepped at 0.20°C intervals from 30°C to 100°C and back to 30°C. During the heating portion in Figure 6, a notable increase in modulus is observed near 69°C, indicative of the stiffening that occurs as the material transforms to austenite. During heating, the damping as shown in Figure 7 decreases at or near the austenite transformation temperature. Above A_f negligible damping exists as there are no twins to absorb energy. Returning to Figure 6, in the cooling portion a sharp decrease in modulus is observed while in Figure 7 an increase in tan δ is observed during cooling. The sharp increase in damping at T = 69°C corresponds to the start of the R-phase of the material. At the start of the R-phase, twins begin to form creating a dramatic decrease in modulus and increase in damping. The largest damping (seen in the martensite phase) is a tan δ of 0.07.

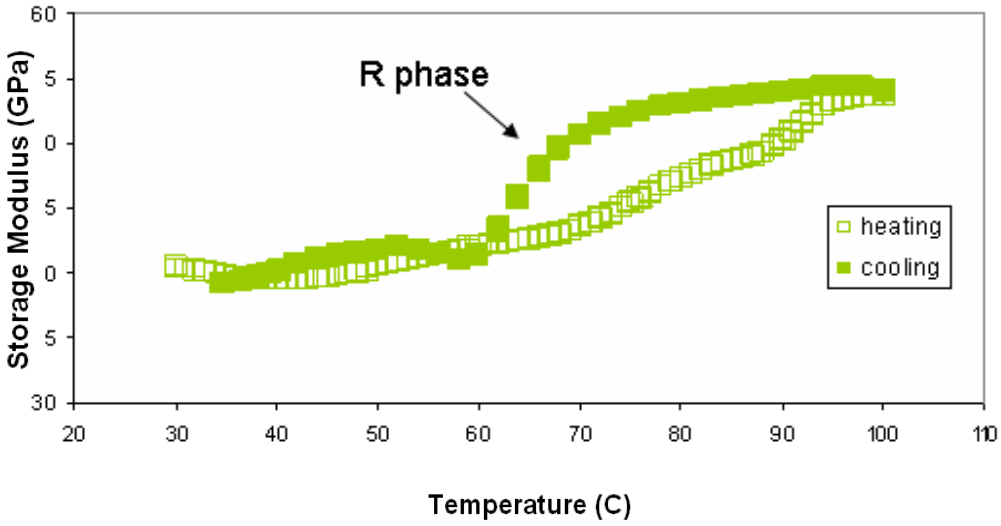

Figure 6: Storage modulus versus temperature for heating and cooling curves.

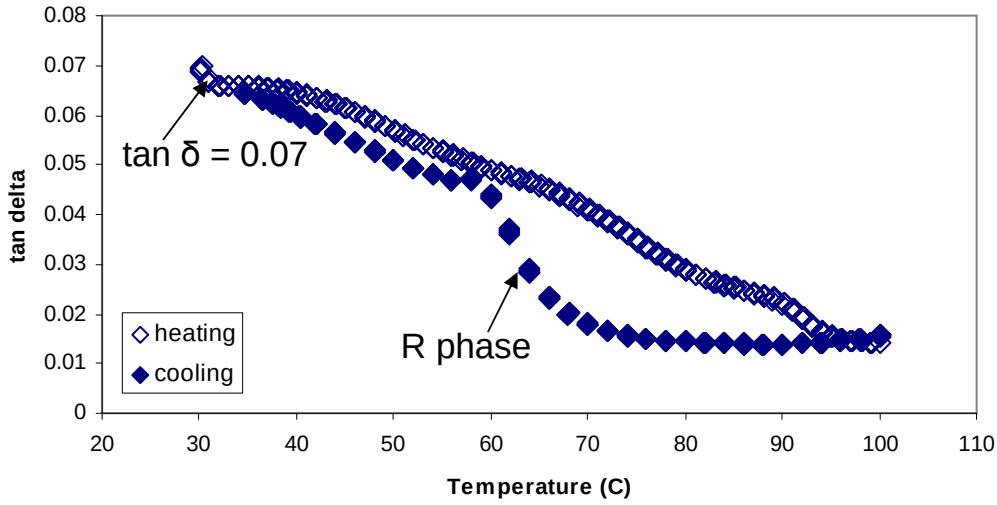

Figure 7: tan δ versus temperature for heating and cooling curves.

Figure 8 shows NiTi thin film modulus and tan δ versus frequency with measurements performed at room temperature with a strain amplitude of 0.20% (figure 3C). This figure shows a relatively constant response in both modulus and tan δ over a frequency range of 0 to 100Hz. Therefore, damping is relatively independent of frequency below 100Hz.

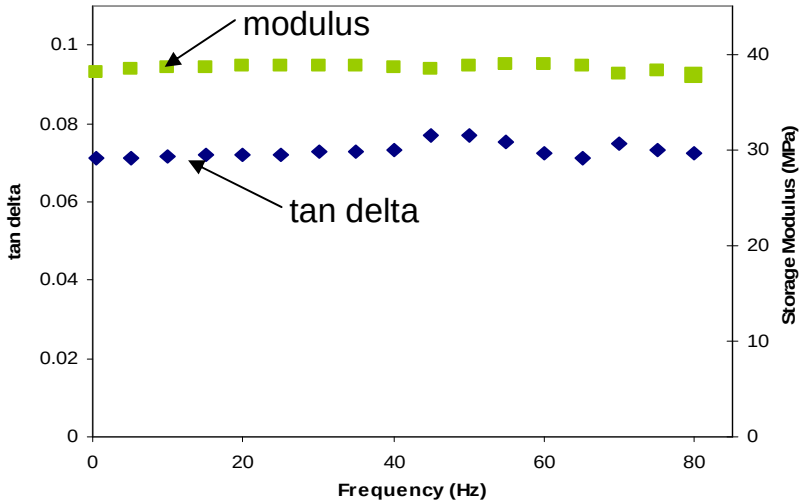

Figure 8: tan δ and storage modulus versus frequency.

While the values of NiTi thin film tan δ presented thus far are acceptable, at first glance they may appear below those of viscoelastic materials. It is important to realize that damping measured under pure tensile loadings is possible due to residual stresses in the film. When the film is placed in tension the twin boundaries move and when the tension is released the residual stresses in the film produce a restoring force to move the twins back. However, when the film is subjected to tensile/compressive load, substantially larger values of tan δ are expected. If the film was integrated into a MEMS device subjected to cyclic bending it would be exposed to tension and compressions loads and thus produce higher damping values than presented in Figure 5 and Figure 7.

Figure 9 provides DMA experimental results for the Nitinol/Silicon/Nitinol beam. Figure 9 plots tan δ data as a function of strain amplitude for the laminate (diamonds) as well as theoretically extracted values for the Nitinol film (squares). The laminate measured tan δ values shows an increasing tan δ with strain amplitude. Due to the brittleness of the silicon, strain values were limited to below 0.27%. The laminate data in Figure 9 was used in equation (15)

along with stiffness properties for the Nitinol (Young's modulus of 28GPa) and silicon (Young's modulus of 150GPa) to back out the Nitinol film tan δ values (i.e. squares). As can be seen in figure 8 the Nitinol thin film has tan δ as large as 0.27 and the damping has not yet saturated. Also, for strain amplitudes below 0.21% there is negligible damping produced from the film. This corresponds to the region below the threshold strain for twin boundary motion (Van Humbeeck, 2003).

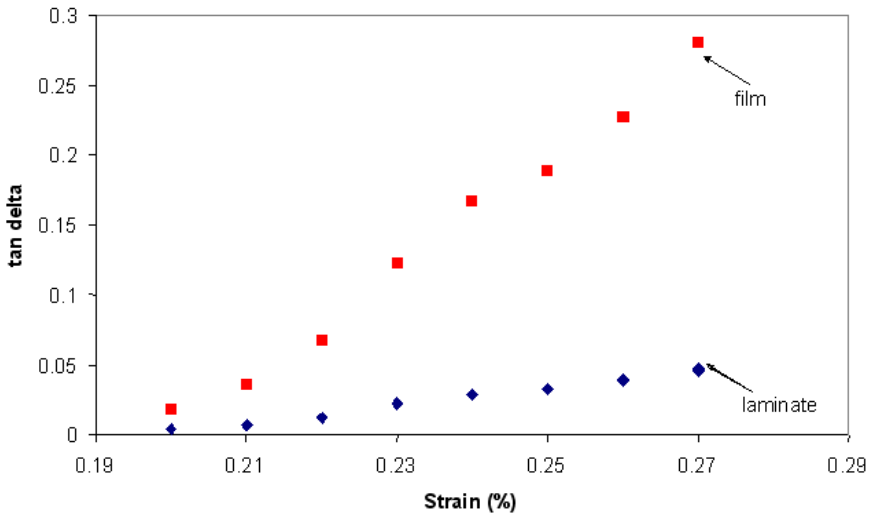

Figure 9: Tan delta versus strain amplitude for the Nitinol/Silicon laminate.

Figure 9 provides DMA experimental results for the Nitinol/Terfenol-D/Nitinol/Nickel/ Nitinol/Terfenol-D/Nitinol beam. Below 0.2% strain, the damping provided by the laminate is attributed to the Terfenol-D layers. Above this strain level, domain wall motion saturates and Terfenol-D should not provide additional damping [5]. At approximately 0.2%, the strain threshold required for martensite reorientation in the Nitinol layers is reached and the Nitinol begins to contribute to damping. As the strain increases above 0.28%, the Nitinol damping continues to increase.

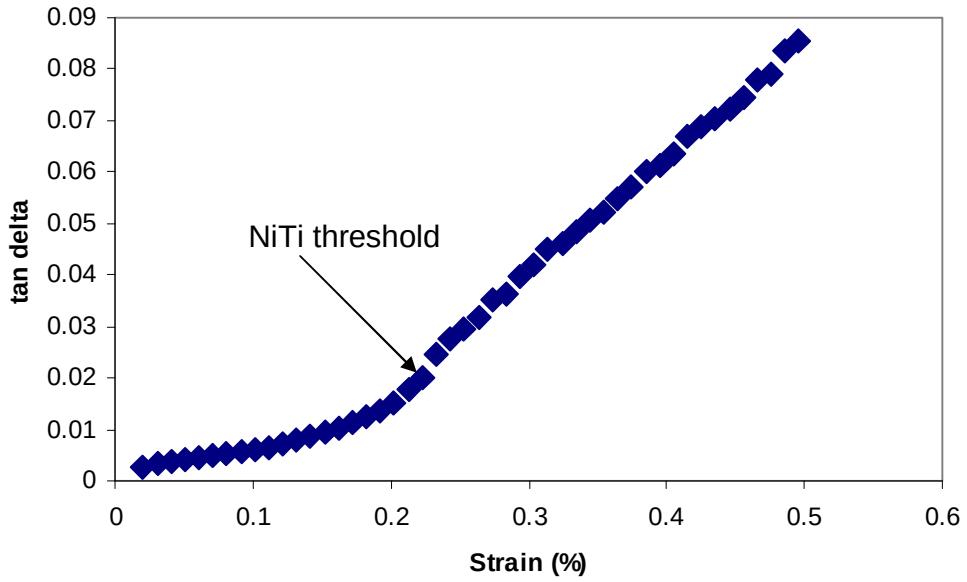

Figure 9: Tan delta versus strain amplitude for the Nitinol/Terfenol-D/Nickel laminate.

Figure 10 provides DMA experimental results for the Nitinol/Terfenol-D/Nitinol/Nickel/ Nitinol/Terfenol-D/Nitinol laminate as presented in figure 9 as well as theoretically calculated values for the Terfenol-D film. The theoretically calculated values were obtained using the tan δ values of Nitinol film provided in figure 8 along with the stiffness properties for Nitinol, nickel and Terfenol-D in equation 15 to back out the Terfenol-D tan δ values (squares). As can be seen, the damping provided by the Terfenol-D layer increases from a very low strain (0.05%) and saturates at a tan δ of 0.21 at 0.2% strain. The tan δ value of 0.21 compares favorably with "bulk" values measured by Ho [6] of 0.29. The Nitinol/Terfenol-D/Nickel laminate was tested at higher strains (i.e 0.5% as shown in Figure 9), however the Terfenol-D film damping could not be extracted at these larger strains as tan δ values of the Nitinol film were limited to 0.27% strain (i.e. see figure 8).

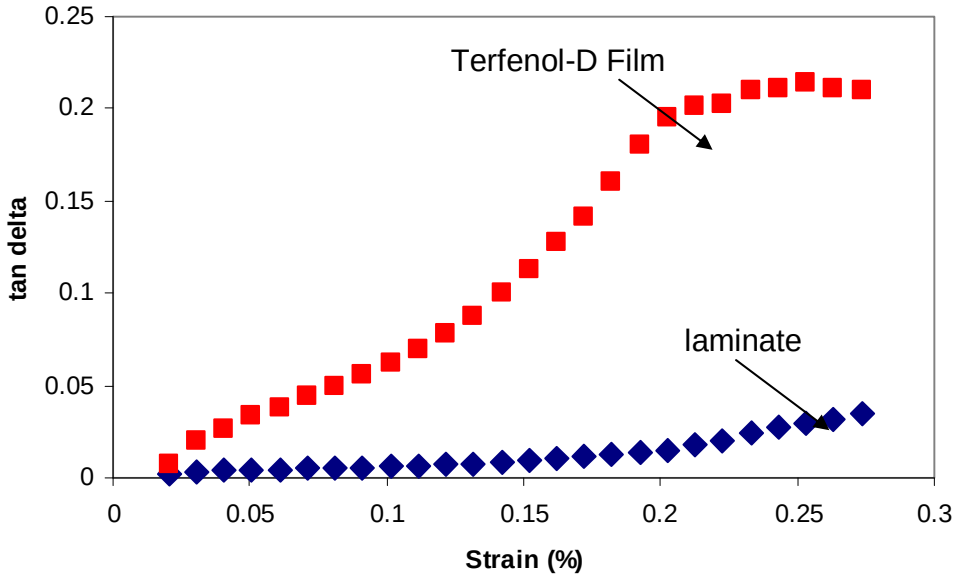

Figure 10: Tan delta versus strain amplitude for the Nitinol/Terfenol-D/Nickel laminate and Terfenol-D film.

Figure 11 shows theoretical predictions of the damping of a symmetric Nitinol/Terfenol-D/Nitinol/Nickel/Nitinol/Terfenol-D/Nitinol laminate as a function of the volume fraction of Terfenol-D and the percent strain as predicted using the developed model (equation 15). The lay up of this laminate was taken to be Nitinol/Terfenol-D/Nitinol/Nickel/Nitinol/Terfenol-D/Nitinol. The volume fraction of Terfenol-D is defined to be the total thickness of the Terfenol-D layers divided by the total thickness of all the damping layers (Terfenol-D and Nitinol). A Terfenol-D volume fraction of one implies that the damping layers consist of Terfenol-D alone, while a volume fraction of zero implies that the damping layers consist of Nitinol alone. The tan δ versus strain amplitude values were obtained from experimental data for thin film Nitinol (Figure 9) and previously published data on bulk Terfenol-D [7]. Figure 11 illustrates how Nitinol and Terfenol-D can be combined to achieve improved damping at both low and high strain amplitudes. At low Terfenol-D volume fraction very little damping is seen at

small strain amplitudes while larger damping is observed at larger strain amplitudes. As the Terfenol-D volume fraction is increased the damping at low strain amplitudes increases. By utilizing a combination of Nitinol and Terfenol-D damping layers the low strain damping can be improved while still maintaining a relatively large tan δ at high strain amplitudes thus producing a broadband damper with relatively constant tan δ for strain values between 0.05% and 1%.

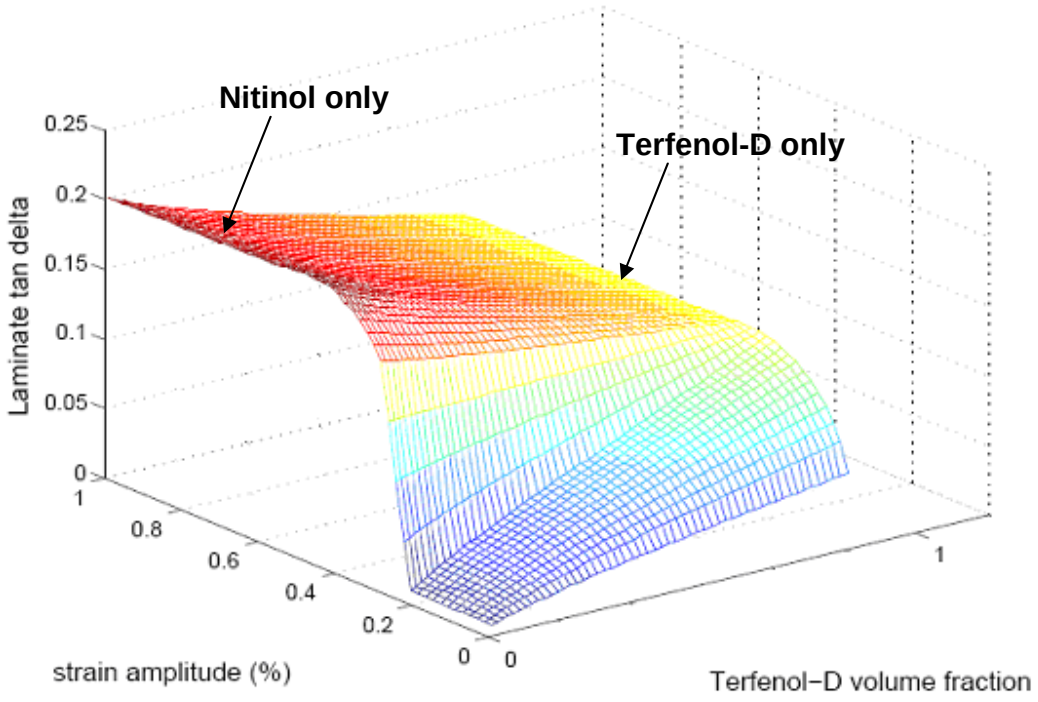

Figure 11: Laminate tan δ versus strain amplitude and Terfenol-D volume fraction.

Figure 12 provides theoretical values of laminate tan δ as a function of stiffness ratio and thickness ratio (equation 15). The hypothetical laminate is composed of a non-damping structural layer coated on either side by a layer of damping material. The damping layer is assumed to have a tan δ of 0.2 (same order as both Terfenol-D and Nitinol). The stiffness ratio is defined as the Young's modulus of the damping layer (E_1) divided by the Young's modulus of

the non-damping structural layer (E_2). The thickness ratio is defined as the thickness of the damping layer (t_1) divided by the thickness of the whole laminate (t_{tot}). As expected the largest thickness ratio results in the largest laminate tan δ. The results in Figure 12 also show that for compliant damping layers (i.e. $E_1/E_2<1$), the damping is severely limited compared to stiff damping layers (i.e. $E_1/E_2>1$). This illustrates the advantages of using stiff layers such as Nitinol and Terfenol-D as compared to viscoelastic layers.

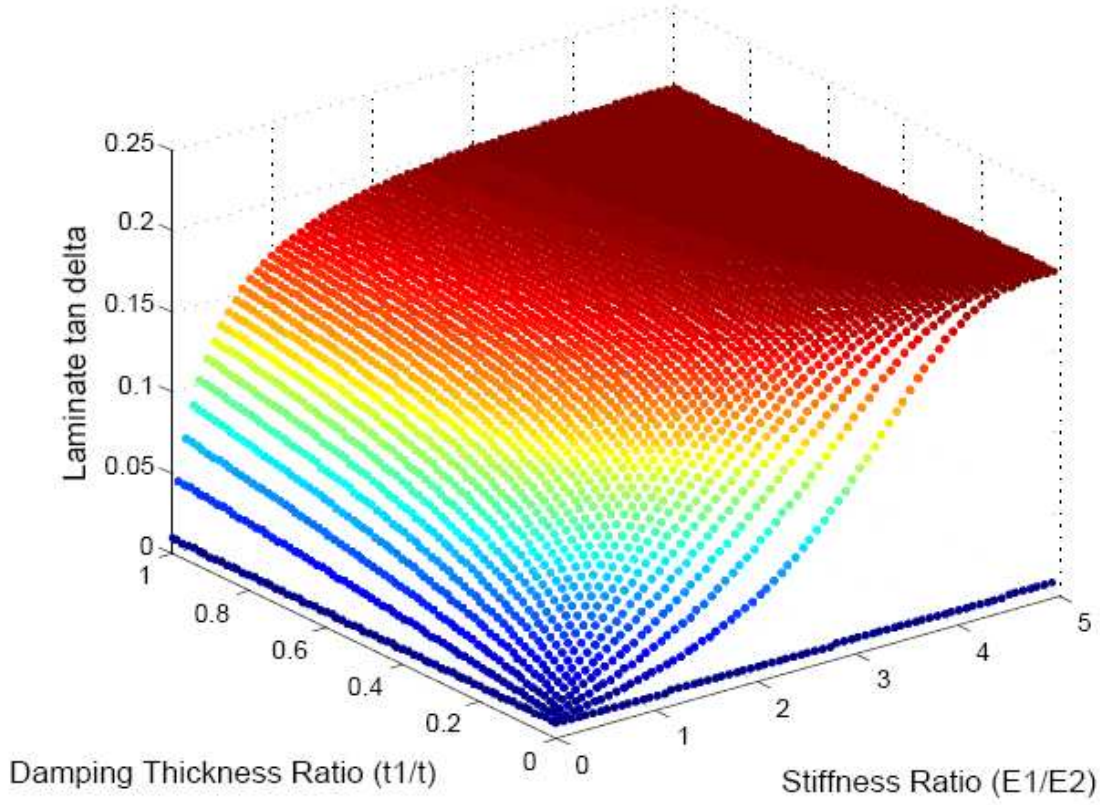

Figure 12: Peak laminate tan delta versus damping layer to substrate layer Stiffness Ratio (E_1/E_2) and damping layer thickness to total thickness ratio (t_1/t_{tot}).

Conclusion

NiTi and Terfenol-D films were successfully deposited by DC magnetron sputtering. A model for prediction of the damping properties (tan δ) of a laminate using the material properties

of the layers was developed. Damping properties in Nitinol thin film due only to residual stresses was measured to be as high as tan $\delta = 0.17$ for large strain (0.9%). At lower strain levels a Nitinol/Silicon laminate was tested in a cantilever load frame. The damping value of the film was measured to be 0.28 (at 0.27% strain). This was a significant improvement over the tensile only loading which exhibited tan $\delta = 0.06$ at the same strain level. A Nitinol/Terfenol-D/Nickel laminate was fabricated and tested in a cantilever loading. The damping value of the film was measured to be 0.2 (at 0.27% strain).

References

1. Ho, K.K.; Mohanchandra, K.P.; Carman, G.P. "Examination of the sputtering profile of NiTi under target heating conditions". Thin Solid Films, vol.413, (no.1-2), Elsevier, 24, p.1-7, (June 2002).
2. Clark, A.E., Abbundi, R., and Gillmor, W.R., "Magnetization and magnetic anisotropy of TbFe2, DyFe2, Tb0.27Dy0.73Fe2 and TmFe2," IEEE Transactions on Magnetics, MAG-14, no.5, p.542-544, (1978).
3. Engdahl, G., Handbook of Giant Magnetostrictive Materials, (2000).
4. McKnight, Geoffrey P., "[112] Oriented Terfenol-D Composites," Ph.D. Thesis, University of California at Los Angeles, 2002.
5. Van Humbeeck, J., Leuven, K.U., "Damping capacity; of thermoelastic martensite in shape memory alloys," Journal of Alloys and compounds, 355, 1-2, p. 58-64, (2003).
6. K.K. Ho, O. Luna, G.P. Carman, and T.A. Duenas, Integrated Ferroelectrics 71, 241 (2005).
7. M. Wun-Fogle, J.B. Restorff, A.E. Clark, and J Snodgrass, IEEE Transactions on Magnetics 39, 3408 (2003).